Inductively coupled plasma sources

J. T. Guðmundsson

Space and Plasma Physics, KTH Royal Institute of Technology, Stockholm, Sweden
Science Institute, University of Iceland, Reykjavik, Iceland
tumi@hi.is

HRMT-62 collaboration meeting @ CERN
September 26., 2022

Introduction

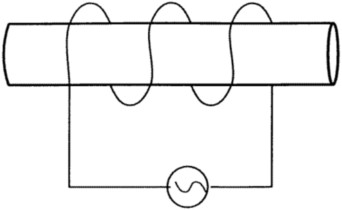

From Gudmundsson and Lieberman (1997) PSST **6** 540

- The inductive discharge in the cylindrical configuration
- In its simplest form it is a tube made of quartz or ceramic placed inside a solenoid (the primary coil) through which rf current is applied
- These discharges have been explored extensively through the years See e.g. Eckert (1986) *Proceedings of the Second Annual International Conference on Plasma Chemistry and Technology*, p. 171 – 202

Introduction

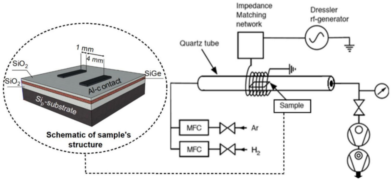

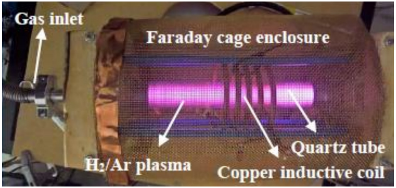

From Sultan (2019)

- We apply an inductively coupled discharge in the cylindrical configuration for hydrogenation of semiconductors

Introduction

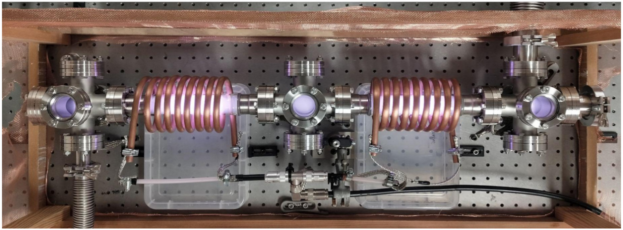

- An inductively coupled discharge in the cylindrical configuration been translated into a plasma cell that is approx 5 cm diameter and 1 m long

Introduction

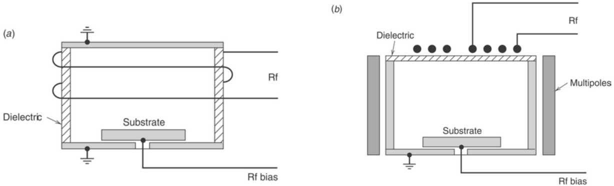

From Lieberman and Lichtenberg (2005)

- The inductively coupled discharge is either in the **cylindrical** or **planar** configuration
- Inductive coils are commonly driven at 13.56 MHz or below, using a 50 Ω rf generator through a capacitive matching network

Introduction

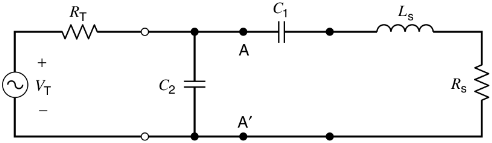

Lieberman and Lichtenberg (2005)

- The high inductive voltage required for the inductive coil can be supplied from a 50 Ω rf generator through a capacitive matching network

Introduction

- Radio frequency (rf) inductively coupled plasma discharges have been studied for over almost 140 years
- Their operation is based on Faraday's law

$$\nabla \times \mathbf{E} = -\frac{\partial \mathbf{B}}{\partial t}$$

- An rf current flowing through an antenna coil induces a time-varying magnetic field which in turn produces an induction field, which generates and sustains the discharge
- This system can be thought of as a transformer circuit in which the antenna coil acts as the primary circuit, while the plasma forms the secondary circuit with a single circular loop

Introduction

- Inductive discharges date back to the first report by Hittorf in 1884
- "I also discoverd a method to send a current through a gas that depends on the inducing action of another current and requires no electrodes at all."
- Hittorf wrapped several turns of insulated wire around a tube and discharged a Leyden jar through it – which caused a flash in the rarefied air

90 *W. Hittorf.*

IV. ***Ueber die Electricitätsleitung der Gase; von W. Hittorf.***

(Fortsetzung von Bd. 20. p. 755.)

§ 6. Weitere Eigenthümlichkeiten des Kathodenlichtes in Gasen von geringer Dichte.

50. Die stetige Ausdehnung, welche das Glimmlicht auf der Oberfläche der Kathode bei Zunahme der Stromstärke nach dem vorigen Paragraphen erfuhr, tritt beim galvanischen Strome, ganz wie beim Inductionsstrome, nur dann ein, wenn die Röhre, in deren Axe der negative Draht liegt, eine genügende Weite hat. Je geringer die Dichte des Gases ist, desto grösser muss der Durchmesser sein.

Auch in dieser Hinsicht darf ich mich auf meine erste Mittheilung beziehen, indem mit einer Ausnahme alle Verhältnisse, welche in § 4 derselben erörtert sind, für den galvanischen Strom gelten.

51. Als Beleg für diese Behauptung möge zunächst eine Versuchsreihe dienen, in welcher zwei cylindrische Röhren mit sehr verschiedenen Durchmessern ($10^1/_2$ cm und 1 cm) und gleichen Electroden, die denselben Abstand von einander hatten, einzeln in den Schliessungsbogen, welcher dieselbe Elementenzahl und die nämliche Widerstandssäule enthielt, abwechselnd aufgenommen wurden. Beim Durchgange des Stromes durch die einzelne Röhre war ihr Gas durch einen Hahn abgesperrt. Aluminiumdrähte von 12 cm Länge und 2 mm Dicke bildeten die Kathoden (c); die Anoden (a) waren Drähte desselben Metalles von derselben Dicke und durch den Abstand (17 mm) von ersteren getrennt (Fig. 7). Die Röhren befanden sich gleichzeitig an der Quecksilberpumpe und enthielten jedesmal Luft von derselben Dichte.

Bemerkungen zu der Tabelle XVI. Bei der Spannkraft der Luft von 1,45 mm (Nr. 1 und 2) und bei grösserer bildet sich das Glimmlicht auf dem Drahte der engen Röhre bedeutend leichter, obgleich beide Drähte aus demselben Stücke ursprünglich genommen waren. Solche Unterschiede kommen, namentlich beim Aluminium, fast immer vor.

Hittorf (1884) *Annalen der Physik* **257** 90 – 139

Introduction

- Hittorf's experiments were picked up by J. J. Thomson and his studies extended almost four decades
- Just like Hittorf, Thomson was convinced that the discharge was formed due to induction phenomenon
- Based on this idea Thomson developed a model of the discharge – which we discuss later
- But the idea that the discharge was due to induction was not accepted by everyone

THE

LONDON, EDINBURGH, AND DUBLIN

PHILOSOPHICAL MAGAZINE

AND

JOURNAL OF SCIENCE.

[FIFTH SERIES.]

OCTOBER 1891.

XLI. *On the Discharge of Electricity through Exhausted Tubes without Electrodes.* By J. J. THOMSON, *M.A., F.R.S., Cavendish Professor of Experimental Physics, Cambridge.**

THE following experiments, of which a short account was read before the Cambridge Philosophical Society last February, were originally undertaken to investigate the phenomena attending the discharge of Electricity through Gases when the conditions are simplified by confining the discharge throughout the whole of its course to the gas, instead of, as in ordinary discharge-tubes, making it pass from metallic or glass electrodes into the gas, and then out again from the gas into the electrodes.

In order to get a closed discharge of this kind we must

Thomson (1891) *Philosophical Magazine, Series 5* **32** 321 – 336, 445 – 464

Introduction

- Nikola Tesla: “Prof. J. J. Thomson’s view of the phenomena under consideration seems to be that they are wholly due to electro-magnetic action. I was, at one time, of the same opinion, but upon carefully investigating the subject I was led to the conviction that they are more of an electrostatic nature.”

  Tesla (1891a) *The Electrical Engineer* **XII**(165) 14–15

- and later “I did not, as Prof. J. J. Thomson seems to believe, misunderstand his position in regard to the cause of the phenomena considered, but I thought that in his experiments, as well as in my own, electrostatic effects were of great importance.”

  Tesla (1891b) *The Electrical Engineer* **XII**(173) 233

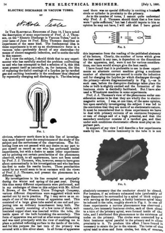
THE ELECTRICAL ENGINEER. [July 1, 1891.

ELECTRIC DISCHARGE IN VACUUM TUBES.

Introduction

LXVI. *On the Origin of the Electrodeless Discharge.*
By K. A. MacKinnon, *M.Sc.**

1. ALTHOUGH the electrodeless discharge was discovered as long ago as 1884, there are still conflicting views regarding its origin. Experimental evidence has been given by many writers (Lehrmann (1), Tesla (2), Lecher (3), Steiner (4), etc.) that the discharge is the result of the large alternating potential differences which exist between the ends of a coil carrying high-frequency currents, while according to Hittorf 5, its discoverer, and to J. J. Thomson (6) the discharge is due to electromagnetic induction. As recently as 1927, Thomson (7), using excitation by spark discharges, has given additional experimental evidence supporting the view which he has always held. This paper was followed by one by Townsend and Donaldson (8 criticizing the electromagnetic view. They point out that theoretically the electrostatic intensity (E_s) between the ends of a solenoidal coil of ordinary dimensions is more than thirty times the electromagnetic intensity (E_m) around a ring inside the coil. Thus they are led to conclude that the electrostatic forces are largely responsible for the electrodeless discharge. In support of this conclusion they give experimental evidence obtained with the use of continuous wave (c.w.) excitation.

From MacKinnon (1929)

- The debate on the workings of the discharge lasted for decades
- But in 1929 MacKinnon explained that electrostatic potential between the coil ends (E mode) preceeded electromagnetic induction (H mode)

Introduction

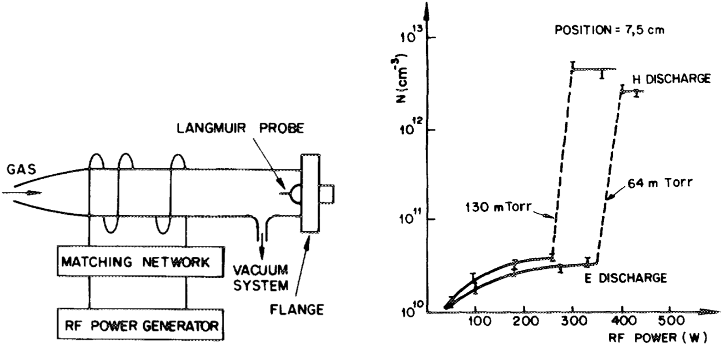

From Amorim et al. (1991) JVSTB **9** 362 – 365

- At low power the discharge operates in E mode and at high power in H mode
- There is a jump in the plasma density when the discharge transitions from E mode to H mode

Introduction

- At low power, a dim discharge is observed (E mode), and on increasing the rf power and coil current, the discharge light emission increases abruptly by almost two orders of magnitude (H mode)
- Emission from the argon 419.8 and 420.0 nm lines in a pure argon discharge at 0.1 Torr as a function of the rf coil current amplitude
- A pronounced hysteresis is observed – which can be due to stepwise ionization and/or a change in the EEDF during the mode transition

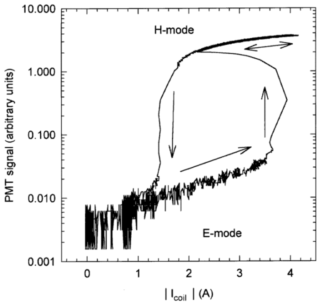

Kortshagen et al. (1996) *Journal of Physics D* **29** 1224

Experimental characterization

Electrostatic probe diagnostics

- A metal probe, inserted in a discharge and biased positively or negatively to draw electron or ion current, is one of the earliest and still one of the most useful tools for diagnosing a plasma.
- These probes, introduced by Irving Langmuir are usually called **Langmuir probes**

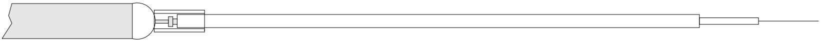

Electrostatic probe diagnostics

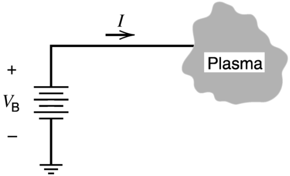

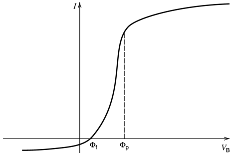

From Lieberman and Lichtenberg (2005).

- At the probe voltage $V_B = \Phi_p$, the probe is at the same potential as the plasma and draws mainly current from the more mobile electrons, which is designated as positive current flowing from the probe into the plasma
- For increasing V_B above this value, the current tends to saturate at the electron saturation current, but, depending on the probe geometry, can increase due to increasing effective collection area

Electrostatic probe diagnostics

- For $V_B < \Phi_p$ electrons are repelled according to the Boltzmann relation, until at Φ_f the probe is sufficiently negative with respect to the plasma that the electron and ion currents are equal such that $I = 0$
- Φ_f is known as the floating potential, because it is the potential at which an insulated probe, which cannot draw current, will float
- For $V_B < \Phi_f$, the current is increasingly ion current (negative into the plasma), tending to an ion saturation current

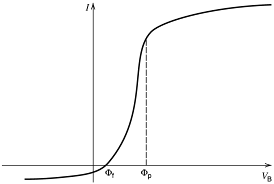

From Lieberman and Lichtenberg (2005)

Electrostatic probe diagnostics

- The electron energy distribution function (EEDF) can be determined from the $I - V$ characteristics

$$g_{\mathrm{e}}(V) = \frac{2m}{e^2 A}\left(\frac{2eV}{m}\right)^{1/2}\frac{\mathrm{d}^2 I_{\mathrm{e}}}{\mathrm{d}V^2} \tag{1}$$

- We often use the electron energy probability function (EEPF)

$$g_{\mathrm{p}}(\mathcal{E}) = \mathcal{E}^{-1/2} g_{\mathrm{e}}(\mathcal{E}) \tag{2}$$

- For a Maxwellian distribution

$$g_{\mathrm{p}}(\mathcal{E}) = \frac{2}{\sqrt{\pi}} n_{\mathrm{e}} \mathrm{T_e}^{-3/2} \exp(-\mathcal{E}/\mathrm{T_e}) \tag{3}$$

such that $\ln g_{\mathrm{p}}$ is a linear function of $\mathcal{E}$

Electrostatic probe diagnostics

- The electron density n_e is then

$$n_{\rm e} = \int_0^\infty g_{\rm e}(\mathcal{E})\,{\rm d}\mathcal{E} \tag{4}$$

and the average energy of electrons

$$\langle \mathcal{E} \rangle = \frac{1}{n_{\rm e}} \int_0^\infty \mathcal{E} g_{\rm e}(\mathcal{E})\,{\rm d}\mathcal{E} \tag{5}$$

- The effective electron temperature is defined as

$$T_{\rm eff} = \frac{2}{3}\langle \mathcal{E} \rangle \tag{6}$$

- The maximum in the first derivative ${\rm d}I_{\rm e}/{\rm d}V_{\rm B}$ of the electron current is also a good indicator for the location of the plasma potential $\Phi_{\rm p}$

Electrostatic probe diagnostics

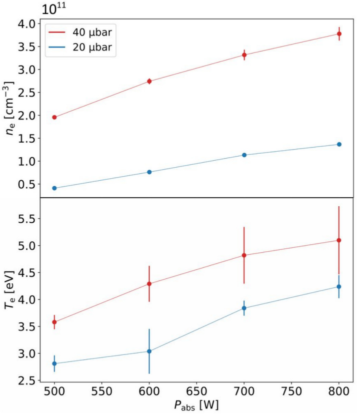

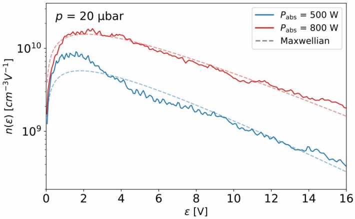

- The measured electron density and electron energy distribution function in the ICP source at 30 and 15 mTorr

Particle and energy balance in discharges

Particle and energy balance

- For low pressure discharges the plasma is not in thermal equilibrium and the electrical power is coupled most efficiently to plasma electrons
- Consider an argon discharge
- In its simplest form argon discharge consists of

$$\mathrm{e}, \mathrm{Ar}, \mathrm{Ar}^{+}, \mathrm{Ar}^{*}$$

- There are electron-atom collisions

$$\mathrm{e} + \mathrm{Ar} \longrightarrow \mathrm{Ar}^{+} + 2\mathrm{e} \qquad \text{(ionization)}$$

$$\mathrm{e} + \mathrm{Ar} \longrightarrow \mathrm{Ar}^{*} + \mathrm{e} \longrightarrow \mathrm{Ar} + \mathrm{e} + \text{photon} \qquad \text{(excitation)}$$

$$\mathrm{e} + \mathrm{Ar} \longrightarrow \mathrm{Ar} + \mathrm{e} \qquad \text{(elastic scattering)}$$

Electropositive plasma equilibrium

- The reactions are described by **rate coefficients**

$$k(\mathrm{T_e}) = \langle \sigma(v_\mathrm{R}) v_\mathrm{R} \rangle = \left(\frac{2e}{m_\mathrm{e}}\right)^{1/2} \int_0^\infty \sigma(\mathcal{E}) \mathcal{E}^{1/2} f(\mathcal{E}) \mathrm{d}\mathcal{E}$$

  where $\sigma(v_\mathrm{R})$ is the cross section and v_R is the relative velocity of colliding particles

- The most important rate coefficients for electron collisons in argon are

k_iz	:	for electron-neutral ionization
k_ex	:	for excitation
k_el	:	for momentum transfer

Electropositive plasma equilibrium

- The electron energy distribution function (EEDF) is usually assumed to be Maxwellian

$$g_{\mathrm{e}}(\mathcal{E}) = \frac{2}{\sqrt{\pi}} \frac{1}{\mathrm{T}_{\mathrm{e}}^{3/2}} \exp\left(-\frac{\mathcal{E}}{\mathrm{T}_{\mathrm{e}}}\right)$$

- We can also assume a general electron energy distribution

$$g_{\mathrm{e}}(\mathcal{E}) = c_1 \mathcal{E}^{1/2} \exp\left(-c_2 \mathcal{E}^x\right)$$

$$c_1 = \frac{1}{\langle \mathcal{E} \rangle^{3/2}} \frac{[\Gamma(\xi_2)^{3/2}]}{[\Gamma(\xi_1)^{5/2}]} \quad \text{and} \quad c_2 = \frac{1}{\langle \mathcal{E} \rangle^x} \frac{[\Gamma(\xi_2)]}{[\Gamma(\xi_1)]^x}$$

where $\xi_1 = 3/2x$ and $\xi_2 = 5/2x$

- Here $x = 1$ and $x = 2$ correspond to Maxwellian and Druyvesteyn electron energy distributions, repectively

Electropositive plasma equilibrium

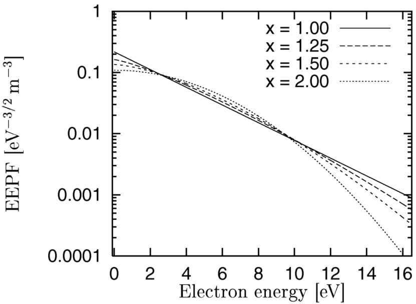

Gudmundsson (2001) PSST **10** 76 – 81

- A plot of the electron energy probability function $g_{\rm p}(\mathcal{E}) = g_{\rm e}(\mathcal{E})\mathcal{E}^{-1/2}$ versus the electron energy

Electropositive plasma equilibrium

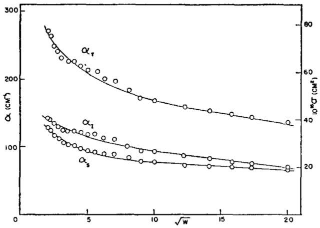

Cramer (1959) Journal of Chemical Physics **30** 641–643

- Argon ions collide with argon atoms

$$\mathrm{Ar}^+ + \mathrm{Ar} \longrightarrow \mathrm{Ar}^+ + \mathrm{Ar} \qquad \text{(elastic scattering)}$$

$$\mathrm{Ar}^+ + \mathrm{Ar} \longrightarrow \mathrm{Ar} + \mathrm{Ar}^+ \qquad \text{(charge transfer)}$$

Electropositive plasma equilibrium

- The total cross section for ions at room temperature

$$\sigma_{\rm i} \approx 10^{-18}\ {\rm m}^2$$

- The ion-neutral mean free path – the distance an ion travels before colliding is

$$\lambda_{\rm i} = \frac{1}{n_{\rm g}\sigma_{\rm i}} = \lambda_{\rm i}\ [{\rm cm}] = \frac{1}{330\ p\ [{\rm Torr}]}$$

where $n_{\rm g}$ is the neutral gas density – $\lambda_{\rm i} \approx 1$ cm at 3 mTorr

- The combined ionic momentum transfer cross section includes charge transfer and eleastic collision

Electropositive plasma equilibrium

- There are three energy loss processes:
  - **Collisional energy** $\mathcal{E}_{\mathrm{c}}$ lost per electron-ion pair created

$$\mathcal{E}_{\mathrm{c}}(\mathrm{T_e}) = \mathcal{E}_{\mathrm{iz}} + \sum_{i=1}^{n} \frac{k_{\mathrm{ex},i}}{k_{\mathrm{iz}}} \mathcal{E}_{\mathrm{ex},i} + \frac{k_{\mathrm{el}}}{k_{\mathrm{iz}}} \frac{3m_{\mathrm{e}}}{M} \mathrm{T_e}$$

  - **Electron kinetic energy** lost to walls

$$\mathcal{E}_{\mathrm{e}} = 2\mathrm{T_e} \quad \text{if Maxwellian EEDF}$$

  - **Ion kinetic energy** lost to walls

$$\mathcal{E}_{\mathrm{i}} \approx \bar{V}_{\mathrm{s}}$$

    or mainly the dc potential across the sheath

Electropositive plasma equilibrium

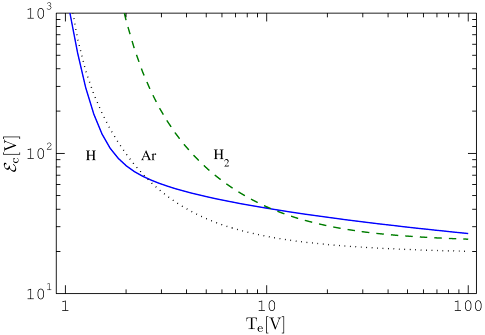

Hjartarson et al. (2010) PSST **19** 065008

- The collisional energy loss per electron-ion pair created for argon, hydrogen atoms and hydrogen molecules assuming Maxwellian EEDF

Electropositive plasma equilibrium

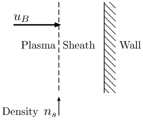

- Ions are lost at the **Bohm velocity** at the plasma-sheath edge

$$u_{\mathrm{i}} = u_{\mathrm{B}} = \left(\frac{k_{\mathrm{B}} T_{\mathrm{e}}}{M} \right)^{1/2}$$

assuming Maxwellian energy distribution or more generally

$$v_{\mathrm{i}} = \langle \mathcal{E} \rangle^{1/2} \left(\frac{2}{M} \right)^{1/2} \frac{[\Gamma(\xi_1)]}{[\Gamma(\xi_2)\Gamma(\xi_3)]^{1/2}}$$

where $\xi_1 = 3/2x$, $\xi_2 = 5/2x$ and $\xi_3 = 1/2x$

Electropositive plasma equilibrium

- At pressures for which the ion loss velocity is the Bohm velocity u_B, the overall discharge power balance for a cylindrical plasma is

$$P_\mathrm{abs} = e n_0 u_\mathrm{B} A_\mathrm{eff} \mathcal{E}_\mathrm{T} \tag{7}$$

where

$$P_\mathrm{abs} : \text{power absorbed by plasma}$$
$$A_\mathrm{eff} : \text{effective area for particle loss}$$

- Loss fluxes to the axial and radial walls are

$$\Gamma_\mathrm{axial} = h_\ell n_0 u_\mathrm{B} \quad \text{and} \quad \Gamma_\mathrm{radial} = h_\mathrm{R} n_0 u_\mathrm{B}$$

Electropositive plasma equilibrium

- There are three regimes we need to take into account:
  - **Low pressure** $\lambda_\mathrm{i} \leq (R, \ell)$. The ion transport is collisionless and well described by an ion free-fall profile within the bulk plasma
    The profile is relatively flat near plasma center and dips near edge,

$$\frac{n_\mathrm{s}}{n_0} \simeq 0.5 \qquad \text{for } R \gg \ell \qquad \text{flat} \tag{8}$$

$$\frac{n_\mathrm{s}}{n_0} \simeq 0.4 \qquad \text{for } \ell \gg R \qquad \text{long cylinder} \tag{9}$$

Electropositive plasma equilibrium

- **Intermediate pressures** $R, \ell \geq \lambda_\mathrm{i} \geq \frac{T_\mathrm{i}}{\mathrm{T_e}}(R, \ell)$.
  The transport is diffusive

$$h_\ell \equiv \frac{n_{\mathrm{s}\ell}}{n_0} \simeq 0.86 \left(3 + \frac{\ell}{2\lambda_\mathrm{i}}\right)^{-1/2} \tag{10}$$

$$h_\mathrm{R} \equiv \frac{n_\mathrm{sR}}{n_0} \simeq 0.80 \left(4 + \frac{R}{\lambda_\mathrm{i}}\right)^{-1/2} \tag{11}$$

- **High pressures** $\lambda_\mathrm{i} < \frac{T_\mathrm{i}}{\mathrm{T_e}}(R, \ell)$
  The transport is diffusive and the density profile is well described by a J_0 Bessel function variation along r and a cosine variation along z

$$h_\ell = \frac{n_\mathrm{sl}}{n_0} \simeq \left[1 + \left(\frac{\ell}{\pi}\frac{u_\mathrm{B}}{D_\mathrm{a}}\right)^2\right]^{-1/2} \tag{12}$$

Electropositive plasma equilibrium

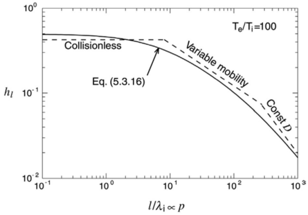

Lieberman and Lichtenberg (2005) and Lee and Lieberman (1995)

- These regimes can be joined heuristically giving

$$h_\ell \approx \frac{0.86}{\left[3 + \ell/2\lambda_\mathrm{i} + (0.86 R u_\mathrm{B}/\pi D_\mathrm{a})^2\right]^{1/2}}$$

$$h_\mathrm{R} \approx \frac{0.8}{\left[4 + R/\lambda_\mathrm{i} + (0.8 R u_\mathrm{B}/\chi_{01} \mathrm{J}_1(\chi_{01}) D_\mathrm{a})^2\right]^{1/2}}$$

Electropositive plasma equilibrium

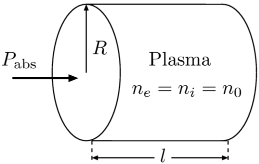

- We assume a uniform cylindrical plasma and the absorbed power is P_{abs}
- Particle balance

$$\underbrace{n_{\mathrm{g}} n_0 k_{\mathrm{iz}} R^2 \ell}_{\text{ionization in the bulk plasma}} = \underbrace{(2\pi R^2 h_\ell n_0 + 2\pi R \ell h_{\mathrm{R}} n_0) u_{\mathrm{B}}}_{\text{ion loss to walls}}$$

Electropositive plasma equilibrium

- Rearrange to obtain

$$\frac{k_{\rm iz}(T_{\rm e})}{u_{\rm B}(T_{\rm e})} = \frac{1}{n_{\rm g} d_{\rm eff}}$$

where

$$d_{\rm eff} = \frac{1}{2} \frac{R\ell}{Rh_\ell + \ell h_R}$$

is an effective plasma size

- So given $n_{\rm g}$ (pressure) and $d_{\rm eff}$ (pressure,dimensions) we know $\mathrm{T_e}$
- The electron temperature is generally in the range 2 – 5 V

Electropositive plasma equilibrium

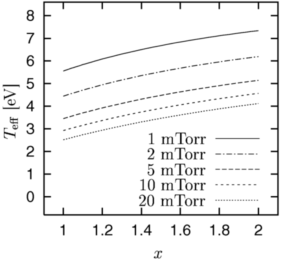

Gudmundsson (2001) PSST **10** 76 – 81

- The effective electron temperature versus x for a cylindrical discharge of radius $R = 15.24$ cm and length $\ell = 7.6$ cm

Electropositive plasma equilibrium

- The power balance is

$$\underbrace{P_{\rm abs}}_{\text{power in}} = \underbrace{(h_\ell n_0 2\pi R^2 + h_{\rm R} n_0 2\pi R\ell) u_{\rm B} e\mathcal{E}_{\rm T}}_{\text{power lost}}$$

- Solve for particle density

$$n_0 = \frac{P_{\rm abs}}{A_{\rm eff} u_{\rm B} e\mathcal{E}_{\rm T}}$$

where

$$A_{\rm eff} = 2\pi R^2 h_\ell + 2\pi R\ell h_{\rm R}$$

is an effective area for particle loss

- Assume low voltage sheaths at all surfaces

$$\mathcal{E}_{\rm T} = \mathcal{E}_{\rm c} + \mathcal{E}_{\rm e} + \mathcal{E}_{\rm i} = \mathcal{E}_{\rm c}({\rm T_e}) + 2{\rm T_e} + 5.2{\rm T_e}$$

Electropositive plasma equilibrium

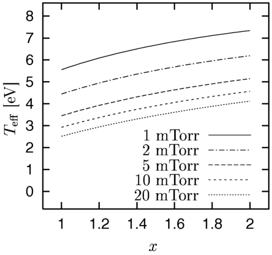

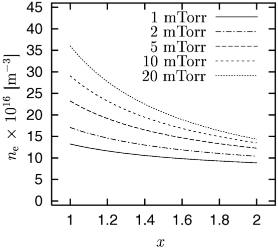

Gudmundsson (2001) PSST **10** 76 – 81

- Particle balance gives the electron temperature
  - only depends on the neutral gas pressure and system dimensions
- Power balance gives the plasma density
  - Once we know the electron temperature

Electropositive plasma equilibrium

Number	Reaction	Rate Constant (m^3/s)	Source
1	e + Ar elastic scattering	$2.336\text{E}{-14}\ T_e^{1.609} \times e^{0.0618(\ln T_e)^2 - 0.1171(\ln T_e)^3}$	a
2	$e + Ar \rightarrow Ar^+ + 2e$	$2.34\text{E}{-14}\ T_e^{0.59}\ e^{-17.44/T_e}$	a
3	$e + Ar \rightarrow Ar^* + e$	$2.48\text{E}{-14}\ T_e^{0.33}\ e^{-12.78/T_e}$	a,b
4	$e + Ar \rightarrow Ar(4s) + e$	$5.0\text{E}{-15}\ T_e^{0.74}\ e^{-11.56/T_e}$	c
5	$e + Ar(4s) \rightarrow Ar + e$	$4.3\text{E}{-16}\ T_e^{0.74}$	d
6	$e + Ar \rightarrow Ar(4p) + e$	$1.4\text{E}{-14}\ T_e^{0.71}\ e^{-13.2/T_e}$	c
7	$e + Ar(4p) \rightarrow Ar + e$	$3.9\text{E}{-16}\ T_e^{0.71}$	d
8	$Ar(4s) + e \rightarrow Ar(4p) + e$	$8.9\text{E}{-13}\ T_e^{0.51}\ e^{-1.59/T_e}$	c
9	$Ar(4p) + e \rightarrow Ar(4s) + e$	$3.0\text{E}{-13}\ T_e^{0.51}$	d
10	$e + Ar(4s) \rightarrow Ar^+ + 2e$	$6.8\text{E}{-15}\ T_e^{0.67}\ e^{-4.20/T_e}$	c
11	$e + Ar(4p) \rightarrow Ar^+ + 2e$	$1.8\text{E}{-13}\ T_e^{0.61}\ e^{-2.61/T_e}$	c
12	$e + Ar_m \rightarrow Ar_r + e$	$2\text{E}{-13}$	c
13	$Ar_r \rightarrow Ar + h\nu$	$3.0\text{E}7\ s^{-1}$	d,e
14	$Ar(4p) \rightarrow Ar + h\nu$	$3.2\text{E}7\ s^{-1}$	d,e

Lieberman and Lichtenberg (2005)

Power absorption – skin depth

Skin depth

- In an inductively coupled plasma source, power is transferred from the electric fields to the plasma electrons within a skin depth layer of thickness δ near the plasma surface
- This is by collisional (Ohmic) dissipation and by collisionless heating process in which the bulk plasma electrons "collide" with the oscillating inductive electric fields within the layer
- The spatial decay constant α within a plasma for an electromagnetic wave normally incident on the boundary of a uniform density plasma is

$$\alpha = \frac{\omega}{c} \mathrm{Im} \left\{ \kappa_{\mathrm{p}}^{1/2} \right\} \equiv \delta^{-1} \tag{13}$$

Skin depth

- From the relative plasma dielectric constant

$$\kappa_{\mathrm{p}} = 1 - \frac{\omega_{\mathrm{pe}}^2}{\omega(\omega - j\nu_{\mathrm{m}})} \simeq -\frac{\omega_{\mathrm{pe}}^2}{\omega^2(1 - j\frac{\nu_{\mathrm{m}}}{\omega})} \tag{14}$$

  we can define three regimes

- $\nu_{\mathrm{m}} \ll \omega$, collisionless

$$\alpha = \frac{\omega_{\mathrm{pe}}}{c} = \frac{1}{\delta_{\mathrm{p}}} \tag{15}$$

$$\delta_{\mathrm{p}} = \left(\frac{m}{e^2 \mu_0 n_{\mathrm{s}}} \right)^{1/2} \tag{16}$$

Skin depth

- $\nu_{\mathrm{m}} \gg \omega$, collisional

$$\alpha = \frac{1}{\sqrt{2}} \frac{\omega_{\mathrm{pe}}}{c} \left(\frac{\omega}{\nu_{\mathrm{m}}} \right) \equiv \frac{1}{\delta_{\mathrm{c}}} \tag{17}$$

and

$$\delta_{\mathrm{c}} = \left(\frac{2}{\omega \mu_0 \sigma_{\mathrm{dc}}} \right)^{1/2} \tag{18}$$

Skin depth

- For $\frac{\overline{v}_{\rm e}}{2\delta_{\rm e}} \gg \omega, \nu_{\rm m}$ a stochastic collision frequency can be defined

$$\nu_{\rm stoc} = \frac{C_{\rm e}\overline{v}_{\rm e}}{\delta_{\rm e}} \tag{19}$$

and

$$\delta_{\rm e} = \frac{c}{\omega_{\rm pe}} \left(\frac{2C_{\rm e}\overline{v}_{\rm e}}{\omega\delta_{\rm e}} \right)^{1/2} \tag{20}$$

or

$$\delta_{\rm e} = \left(\frac{2C_{\rm e}c^2\overline{v}_{\rm e}}{\omega\omega_{\rm e}^2} \right) = \left(\frac{2C_{\rm e}\overline{v}_{\rm e}}{\omega\delta_{\rm p}} \right)^{1/3} \delta_{\rm p} \tag{21}$$

is the anomalous skin depth and $C_{\rm e} \simeq 1/4$.

Transformer model

Discharge operation and coupling

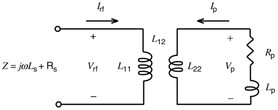

Lieberman and Lichtenberg (2005)

- The inductive plasma source can be modeled as a transformer
- Evaluating the inductance matrix for this transformer, defined through

$$\tilde{V}_{\mathrm{rf}} = j\omega L_{11}\tilde{I}_{\mathrm{rf}} + j\omega L_{12}\tilde{I}_{\mathrm{p}}$$

$$\tilde{V}_{\mathrm{p}} = j\omega L_{21}\tilde{I}_{\mathrm{rf}} + j\omega L_{22}\tilde{I}_{\mathrm{p}}$$

where the tildes denote the complex amplitudes

Discharge operation and coupling

- Assume a uniform density cylindrical discharge in the geometry $\ell \geq R$.

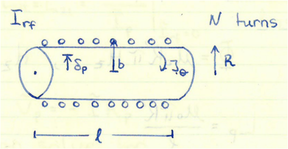

- Assume $\mathcal{N}$ turn coil of radius $b > R$
- The power absorbed by the plasma is

$$P_{\rm abs} = \frac{1}{2}\frac{J_\theta^2}{\sigma_{\rm dc}} 2\pi R \ell \delta_{\rm p} \tag{22}$$

and the plasma current

$$I_{\rm p} = J_\theta \ell \delta_{\rm p} \tag{23}$$

Discharge operation and coupling

- Here J_θ is the amplitude of the induced rf azimuthal current density at the plasma edge near $r = R$ (opposite in direction to the applied azimuthal current in the coil)
- The effective conductivity is

$$\sigma_{\mathrm{eff}} = \frac{e^2 n_{\mathrm{s}}}{m\nu_{\mathrm{eff}}}$$

  with $\nu_{\mathrm{eff}} = \nu_{\mathrm{stoc}} + \nu_m$ a sum of collisional and stochastic heating
- Letting $I_{\mathrm{p}} = J_\theta l\delta$ to be the total induced rf current amplitude in the plasma skin and defining the plasma resistance through

$$P_{\mathrm{abs}} = \tfrac{1}{2} I_{\mathrm{p}}^2 R_{\mathrm{p}} \tag{24}$$

Discharge operation and coupling

- Thus we have the plasma resistance

$$R_{\rm p} = \frac{2\pi R}{\sigma_{\rm dc}\ell\delta_{\rm p}} \tag{25}$$

- The plasma inductance is found by using

$$\Phi = L_{22} I_{\rm p} = \mu_0 R^2 \pi H_z \tag{26}$$

where

$$H_z = J_\theta \delta_{\rm p} \tag{27}$$

thus

$$L_{22} = \frac{\mu_0 \pi R^2}{\ell} \tag{28}$$

Discharge operation and coupling

- The voltage applied to the coil is

$$\overline{V}_{\rm rf} = j\omega L_{11}\tilde{I}_{\rm rf} + j\omega L_{12}\tilde{I}_{\rm p} \tag{29}$$

where

$$L_{11} = \left.\frac{\Phi}{I_{\rm rf}}\right|_{\tilde{I}_{\rm rf}=0} = \frac{\mathcal{N}^2\mu_0\pi b^2}{\ell} \tag{30}$$

and

$$M = L_{12} = L_{21} = \left.\frac{\phi_{\rm coil}}{\tilde{I}_{\rm p}}\right|_{\tilde{I}_{\rm rf}} = \frac{\mu_0\pi R^2\mathcal{N}}{\ell} \tag{31}$$

- Earlier we had

$$L_{22} = \left.\frac{\Phi_{\rm p}}{I_{\rm p}}\right|_{\tilde{I}_{\rm rf}=0} = \mu_0\frac{\pi R^2}{\ell} \tag{32}$$

Discharge operation and coupling

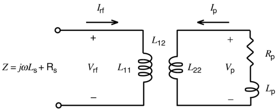

Lieberman and Lichtenberg (2005)

- To describe the plasma use

$$\tilde{V}_{\mathrm{p}} = -\tilde{I}_{\mathrm{p}}(R_{\mathrm{p}} + j\omega L_{\mathrm{p}}) \tag{33}$$

whith

$$L_{\mathrm{p}} = \frac{R_{\mathrm{p}}}{\nu_{\mathrm{eff}}} \tag{34}$$

due to phase lag between the rf electric field and the conduction current

Discharge operation and coupling

- Solve for impedance seen at the primary

$$Z_s = \frac{\tilde{V}_{rf}}{\tilde{I}_{rf}} = j\omega L_{11} + \frac{\omega^2 M^2}{R_p + j\omega(L_{22} + L_p)} \tag{35}$$

so

$$L_s = \frac{\mu_0 \pi R^2 \mathcal{N}^2}{\ell}\left(\frac{b^2}{R^2} - 1\right) \tag{36}$$

if $R_p^2 + \omega^2 L_p^2 \ll \omega^2 L_{22}^2$ and

$$R_s \simeq \mathcal{N}^2 \frac{2\pi R}{\sigma_{eff}\ell\delta_p} \tag{37}$$

- Then

$$P_{abs} = \frac{1}{2}|I_{rf}|^2 R_s \tag{38}$$

Discharge operation and coupling – low density

- At low densities when $\delta \geq R$ the conductivity is low and the fields fully penetrate the plasma
- In this case, applying Farday's law to determine E_θ within the coil

$$\oint_C E \, \mathrm{d}\ell = -\frac{\mathrm{d}\Phi}{\mathrm{d}t} \tag{39}$$

so

$$2\pi r E_\theta(r) = -j\omega\mu_0 \frac{\mathcal{N} I_{\mathrm{rf}}}{\ell} \pi r^2 \tag{40}$$

or

$$E_\theta(r) = -\tfrac{1}{2} j\omega r \mu_0 \mathcal{N} I_{\mathrm{rf}}/\ell \tag{41}$$

Discharge operation and coupling – low density

- Then the induced current is

$$J_\theta = j\omega\epsilon_0\kappa_\mathrm{p}E_\theta \tag{42}$$

and if $\nu_\mathrm{m} \ll \omega$

$$J_\theta \propto n_0 r I_\mathrm{rf} \tag{43}$$

- The power absorbed

$$\begin{aligned}
P_\mathrm{abs} &= \frac{1}{2}\int_0^R \frac{J_\theta^2(r)2\pi r\ell}{\sigma_\mathrm{eff}}\mathrm{d}r && (44)\\
&= \frac{1}{2}I_\mathrm{rf}^2\frac{\pi e^2 n_0 \nu_\mathrm{eff}\mu_0^2\mathcal{N}^2R^4}{8m\ell} && (45)\\
&\propto n_0 I_\mathrm{rf}^2 && (46)
\end{aligned}$$

Discharge operation and coupling

- To estimate the rf voltage across the sheath, $\tilde{V}_{\mathrm{sh}}$, at the high-voltage end of the coil, we note that the sheath capacitance per unit area is $\sim \epsilon_0/s_{\mathrm{m}}$ and the capacitance per unit area of the dielectric cylinder is $\sim \epsilon_0/(b-R)$
- Assuming that the plasma is at ground potential, then the voltage across the sheath is found from the capacitive voltage divider formula,

$$\tilde{V}_{\mathrm{sh}} = V_{\mathrm{rf}} \frac{s_{\mathrm{m}}}{b - R + s_{\mathrm{m}}}$$

Discharge operation and coupling

- Using the modified Child law, we calculate the sheath thickness from

$$e n_{\mathrm{s}} u_{\mathrm{B}} = 0.82 \epsilon_0 \left(\frac{2e}{M} \right)^{1/2} V_{\mathrm{rf}}^{3/2} \left(\frac{s_{\mathrm{m}}}{b - R - s_{\mathrm{m}}} \right)^{3/2} \frac{1}{s_{\mathrm{m}}^2}$$

  which is a cubic equation in s_{m}
- However, for high densities for which $s_{\mathrm{m}} \ll b - R$ this simplifies to

$$s_{\mathrm{m}} \approx \left(\frac{0.82 \epsilon_0}{e n_{\mathrm{s}} u_{\mathrm{B}}} \right) \left(\frac{2e}{M} \right) \frac{V_{\mathrm{rf}}^3}{(b - R)^3}$$

- s_{m} in an inductively coupled discharge is much smaller than in a capacitive discharge

Electromagnetic modeling

Electromagnetic modeling

- In the inductive mode the gas discharge is sustained by induction from a time-varying magnetic field
- Within the plasma, however, the primary field is attenuated exponentially, characterized by the penetration depth or skin depth of the plasma
- Assuming a discharge tube where $\ell \gg R$ we follow the early derivations of Thomson

Thomson (1891) *Philosophical Magazine, Series 5* **32** 321 – 336, 445 – 464

Thomson (1927) *Philosophical Magazine, Series 7* **4** 1128 – 1160

- Maxwell's equations for a medium of dielectric constant $\epsilon = \epsilon_0 \epsilon_{\rm p}$ in cylindrical coordinates reduce to

$$\frac{dH_z}{dr} = -{\rm j}\omega\epsilon E_\theta$$

and

$$\frac{1}{r}\frac{d}{dr}(rE_\theta) = -j\omega\mu_o H_z$$

Electromagnetic modeling

- The plasma dielectric constant is

$$\epsilon_{\rm p} = 1 - \frac{\omega_{\rm pe}^2}{\omega(\omega_{\rm eff} - {\rm j}\nu_{\rm eff})}$$

- In the limit that the that the displacement current $j\omega\epsilon_o\mathbf{E}$ is small compared to the conduction current we can write

$$\frac{dH_z}{dr} = -\sigma E_\theta$$

- Eliminating H_z from the equations we obtain

$$\frac{1}{r}\frac{d}{dr}\left(r\frac{dE_\theta}{dr}\right) - \left(\frac{1}{r^2} - {\rm j}\omega^2\mu_o\epsilon_0\epsilon_{\rm p}(r)\right)E_\theta = 0$$

Electromagnetic modeling

- For an inductive discharge in the in the cylindrical configuration the boundary conditions are $E_\theta(r=0)=0$ and $E_\theta(r=R)=E_{o\theta}$
- The electric field amplitude at the radial boundary $E_{o\theta}$ is found from the power balance within the discharge
- The power density at a radius r is

$$p_{\mathrm{abs}}(r) = \frac{1}{2}\mathrm{Re}[\sigma(r)](E_\theta(r))^2$$

and the total power absorbed in the discharge

$$P_{\mathrm{abs}} = 2\pi L \int_0^R p_{\mathrm{abs}}(r) r dr$$

from which we can find the electric field amplitude at the sheath edge $E_{o\theta}$ for a given absorbed power

Electromagnetic modeling

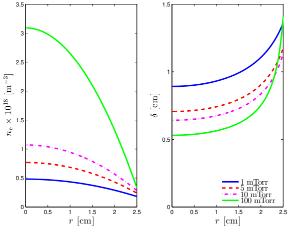

$P_{abs} = 300$ W, $\ell = 30$ cm and $R = 2.5$ cm

- We improve on the assumption of a uniform density and assume a parabolic electron density profile

$$h(r) = (h_R - 1)\frac{r^2}{R^2} + 1$$

is the normalized electron density within the discharge, n_0 is the centre density

$$h(r) = \frac{n(r)}{n_0}$$

Electromagnetic modeling

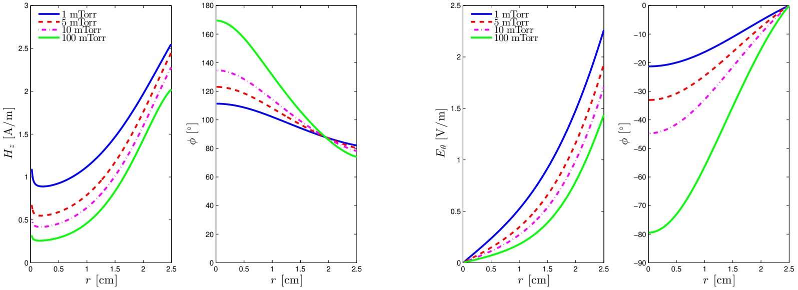

$P_{\text{abs}} = 300$ W, $\ell = 30$ cm and $R = 2.5$ cm

- The magnetic field along the discharge axis and the azimuthal electric field

Electromagnetic modeling

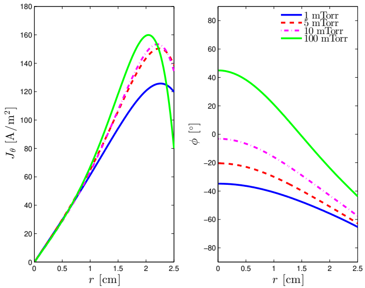

$P_{\text{abs}} = 300$ W, $\ell = 30$ cm and $R = 2.5$ cm

- From Ohm's law, knowing the azimuthal electric field and the plasma conductance, the current density at radius r is

$$J_\theta(r) = |\sigma(r)E_\theta(r)|$$

The planar configuration

Planar configuration

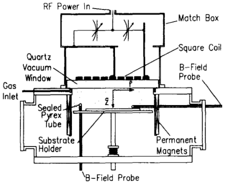

From Hopwood et al. (1993a) JVSTA **11** 147 – 151

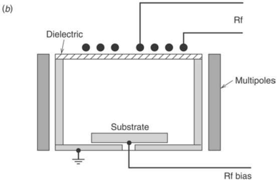

From Lieberman and Lichtenberg (2005)

- The inductively coupled plasma discharge in the planar coil configuration typically generates relatively uniform low aspect ratio plasmas with densities between 10^{17} and 10^{18} m^{-3} over substrate diameters of 20 cm or more

Planar configuration

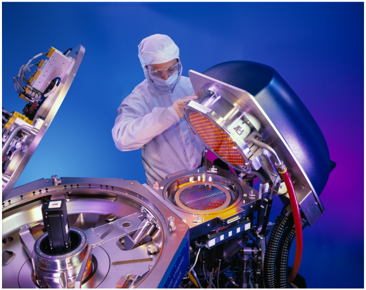

- The inductively coupled plasma discharge in the planar coil configuration is a commonly used for materials processing

Planar configuration

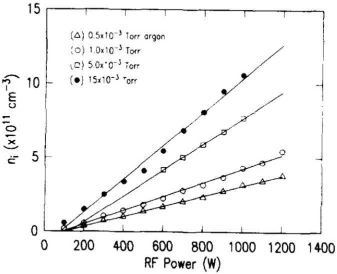

From Hopwood et al. (1993b) JVSTA **11** 152 – 156

- The ion density as a function of power for a planar inductive discharge in argon and krypton

Planar configuration

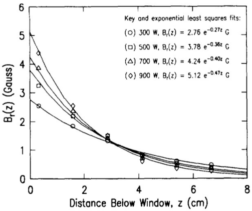

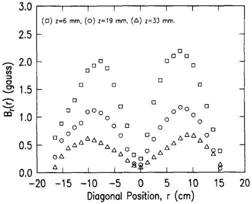

From Hopwood et al. (1993a) JVSTA **11** 147 – 151

- In axisymmetric geometry, the coil generates an inductive field having magnetic components $H_r(r,z)$ and $H_z(r,z)$, and an electric component $E_\theta(r,z)$

Planar configuration

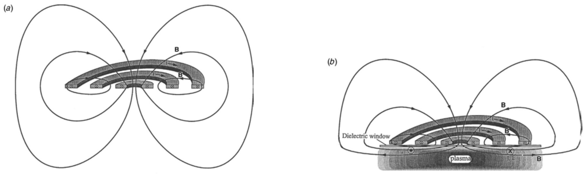

From Lieberman and Lichtenberg (2005) or originally from Wendt (1997)

- When a plasma is formed below the coil, then from Faraday's law an azimuthal electric field E_θ and an associated current density J_θ are induced within the plasma
- The plasma current, opposite in direction to the coil current, is confined to a layer near the surface having a thickness of order the skin depth δ

Planar configuration

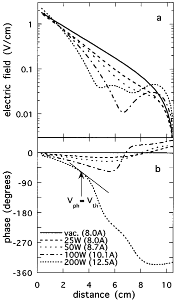

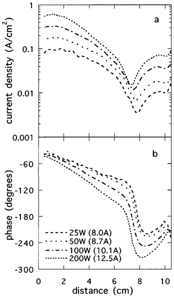

1 mTorr argon from Godyak and Piejak (1997) JAP **82**(12) 5944–5947

- Two-dimensional, phase resolved magnetic probe measurements in a low pressure inductively coupled cylindrical plasma source driven with a planar coil

Planar configuration

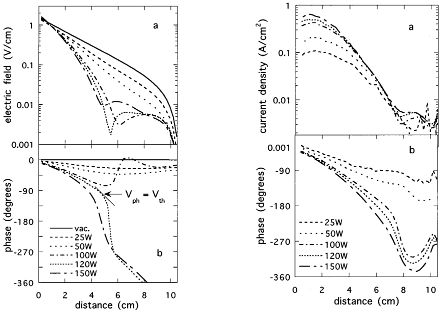

10 mTorr argon from Godyak and Piejak (1997) JAP **82**(12) 5944–5947

- The rf electric field and current density distributions determined from these measurements exhibit an abnormal nonmonotonic spatial evolution – anomalous skin effect

Planar configuration

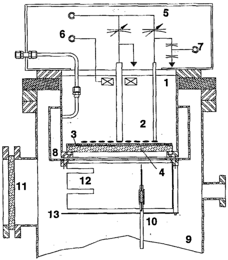

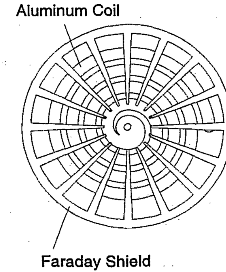

From Mahoney et al. (1994) JAP **76** 2041 – 2047

- Sometimes an electrostatic shield (Faraday shield) placed between the coil and the plasma further reduces the capacitively coupling if desired, which allowing the inductive field to couple unhindered to the plasma

Thank you for your attention

The slides can be downloaded at

`http://langmuir.raunvis.hi.is/∼tumi/ranns.html`

Amorim, J., H. S. Maciel, and J. P. Sudamo (1991). High-density plasma mode of an inductively coupled radio frequency discharge. *Journal of Vacuum Science and Technology B 9*(2), 362 – 365.

Cramer, W. H. (1959). Elastic and inelastic scattering of low-velocity ions: Ne^+ in A, A^+ in Ne, and A^+ in A. *Journal of Chemical Physics 30*(3), 641–643.

Eckert, H. U. (1986). The hundred year history of induction discharges. In H. Boenig (Ed.), *Proceedings of the Second Annual International Conference on Plasma Chemistry and Technology*, Lancaster PA, pp. 171 – 202. Technomic Publishing.

Godyak, V. A. and R. B. Piejak (1997). Electromagnetic field structure in a weakly collisional inductively coupled plasma. *Journal of Applied Physics 82*(12), 5944–5947.

Gudmundsson, J. T. (2001). On the effect of the electron energy distribution on the plasma parameters of argon discharge: A global (volume averaged) model study. *Plasma Sources Science and Technology 10*(1), 76–81.

Gudmundsson, J. T. and M. A. Lieberman (1997). Magnetic induction and plasma impedance in a cylindrical inductive discharge. *Plasma Sources Science and Technology 6*(4), 540–550.

Hittorf, W. (1884). Ueber die Electricitätsleitung der Gase. *Annalen der Physik 257*(1), 90–139.

Hjartarson, A. T., E. G. Thorsteinsson, and J. T. Gudmundsson (2010). Low pressure hydrogen discharges diluted with argon explored using a global model. *Plasma Sources Science and Technology 19*(6), 065008.

References

Hopwood, J., C. R. Guarnieri, S. J. Whitehair, and J. J. Cuomo (1993a). Electromagnetic fields in a radio-frequency induction plasma. *Journal of Vacuum Science and Technology A 11*(1), 147–151.

Hopwood, J., C. R. Guarnieri, S. J. Whitehair, and J. J. Cuomo (1993b). Langmuir probe measurements of a radio frequency induction plasma. *Journal of Vacuum Science and Technology A 11*(1), 152–156.

Kortshagen, U., N. D. Gibson, and J. E. Lawler (1996). On the E-H-mode transition in inductively coupled rf plasmas. *Journal of Physics D: Applied Physics 29*(5), 1224 – 1236.

Lee, C. and M. A. Lieberman (1995). Global model of Ar, O_2, Cl_2 and Ar/O_2 high-density plasma discharges. *Journal of Vacuum Science and Technology A 13*(2), 368–380.

Lieberman, M. A. and A. J. Lichtenberg (2005). *Principles of Plasma Discharges and Materials Processing* (2 ed.). New York: John Wiley & Sons.

MacKinnon, K. (1929). On the origin of the electrodeless discharge. *Philosophical Magazine Series 7 8*(52), 605–616.

Mahoney, L. J., A. E. Wendt, E. Barrios, C. J. Richards, and J. L. Shohet (1994). Electron-density and energy distributions in a planar inductively coupled discharge. *Journal of Applied Physics 76*(4), 2041–2047.

Sultan, M. T. (2019). *Highly photoconductive oxide films functionalized with GeSi nanoparticles*. Ph. D. thesis, Reykjavik University.

Tesla, N. (1891a). Electric discharge in vacuum tubes. *The Electrical Engineer 12*(165), 14–15.

Tesla, N. (1891b). Electric discharge in vacuum tubes. *The Electrical Engineer 12*(173), 233.

Thomson, J. J. (1891). On the discharge of electricity through exhausted tubes without electrodes. *Philosophical Magazine Series 5 32*(197), 321–336.

Thomson, J. J. (1927). The electrodeless discharge through gases. *Philosophical Magazine Series 7 4*(25), 1128–1160.

Wendt, A. E. (1997). The physics of inductively coupled plasma sources. *AIP Conference Proceedings 403*, 435–442.